The Astrophysical Journal, 856:40 (8pp), 2018 March 20 https://doi.org/10.3847/1538-4357/aaaeb8

The Lithium Depletion Boundary and the Age of the Hyades Cluster*

Eduardo L. Martín[1], Nicolas Lodieu[2,3], Yakiv Pavlenko[4], and Víctor J. S. Béjar[2,3]
[1] Centro de Astrobiología (INTA-CSIC), Carretera de Ajalvir km 4, E-28550 Torrejón de Ardoz, Madrid, Spain; ege@cab.inta-csic.es
[2] Instituto de Astrofísica de Canarias (IAC), Calle Vía Láctea s/n, E-38200 La Laguna, Tenerife, Spain
[3] Departamento de Astrofísica, Universidad de La Laguna (ULL), E-38205 La Laguna, Tenerife, Spain
[4] Main Astronomical Observatory of the National Academy of Sciences of Ukraine, Ukraine
Received 2017 June 30; revised 2018 February 8; accepted 2018 February 8; published 2018 March 22

Abstract

Determination of the lithium depletion boundary (LDB), i.e., the observational limit below which the cores of very low-mass objects do not reach high enough temperatures for Li destruction, has been used to obtain ages for several open clusters and stellar associations younger than 200 Myr—which until now has been considered the practical upper limit on the range of applicability of this method. In this work, we show that the LDB method can be extended to significant older ages than previously thought. Intermediate resolution optical spectra of six L-type candidate members in the Hyades cluster obtained using Optical System for Imaging and Low Resolution Integrated Spectroscopy at the 10.4 m Gran Telescopio Canarias are presented. The Li I 670.8 nm resonance doublet is clearly detected only in the two faintest and coolest of these objects, which are classified as L3.5 to L4 brown dwarf (BD) cluster members with luminosities around 10^{-4} solar. Lithium depletion factors are estimated for our targets with the aid of synthetic spectra and they are compared with predictions from evolutionary models. An LDB age of 650 ± 70 Myr for the Hyades provides a consistent description of our data using a set of state-of-the-art evolutionary models for BDs calculated by Baraffe et al.

Key words: brown dwarfs – methods: observational – open clusters and associations: individual (Hyades) – stars: abundances – techniques: spectroscopic

1. Introduction

The light element lithium (Li) is destroyed by collisions with protons in the cores of stars and high-mass brown dwarfs (BDs) with masses above 0.05 $M_{\odot}$ in timescales shorter than 1 Gyr (Magazzù et al. 1993). This nuclear process becomes observable as Li depletion in the surface via deep convective mixing. The discovery of Li in BD members in the Pleiades cluster (Basri et al. 1996; Rebolo et al. 1996) was an observational confirmation that this light element is preserved in substellar mass objects as originally proposed by Rebolo et al. (1992). The first attempt to detect Li in very low-mass members in open clusters (Hyades and Pleiades) was reported in Martín et al. (1994). Currently, the so-called Li test for BD candidates keeps on being used to constrain the ages and masses of young BDs in the field (Phan-Bao et al. 2017).

The Li depletion boundary (LDB) in young open clusters is a chronometer that provides age estimates independent from other methods, such as turn off determination or main-sequence isochrone fitting. The physics involved in using the LDB are considered simpler than other methods used for dating clusters and associations (Burke et al. 2004). However, it has been considered that the LDB method is limited in its practical applicability to the age range between 20 and 200 Myr, which implies that so far it could be used only in two stellar associations and seven young open clusters (Stauffer et al. 1998; Barrado y Navascués et al. 2004; Cargile et al. 2010; Dobbie et al. 2010; Jeffries et al. 2013). In this work, we search for the LDB in the Hyades cluster, and we show that this method can be extended to significantly older ages than previously thought.

Located at only 46.3 ± 0.3 pc, the Hyades is the nearest open cluster (van Leeuwen 2009). The isochrone age usually adopted for this cluster is 625 ± 50 Myr (Maeder & Mermilliod 1981), although a much older age of 1200 Myr has been reported using evolutionary models with enhanced convective overshooting (Mazzei & Pigatto 1988). A recent estimate of the Hyades age using models that incorporate rotation has given 750 ± 100 Myr (Brandt & Huang 2015). Both convective overshooting and stellar rotation increase main-sequence lifetimes and thus yield older cluster ages. The Hyades cluster may be part of larger complex that also includes the Praesepe open cluster and a large number of field stars. This complex, known as Hyades supercluster, includes stellar populations with ages ranging from 0.5 to 1.0 Gyr (Eggen 1998).

Even though the Hyades has a paucity of low-mass members with respect to younger clusters (Reid 1992), which is understood as evidence for dynamical evolution, which makes the lowest mass members disperse from the cluster core (Terlevich 1987), a dozen L dwarf candidates with high probability of membership in the Hyades cluster were identified from photometry and proper motion data presented in Hogan et al. (2008). Moreover, T dwarf candidate members were found by Bouvier et al. (2008), and a late L dwarf member was recently reported in Perez Garrido et al. (2017).

Hyades BDs are benchmarks for understanding substellar evolution and they also provide a unique opportunity to extend the LDB method to a stellar cluster older than 200 Myr. In this paper, we present a search for the Li I resonance doublet centered at 670.8 nm in six L dwarfs selected on the basis of confirmed L-type spectral classification from reconnaissance spectra presented in Lodieu et al. (2014).

* Based on data obtained at the Gran Telescopio Canarias.

Table 1
Observing Log

Abridged Names[a]	2MASS Coordinates	Date	Exposure Time[b] (s)	Seeing[c] (arcsec)	Weather Conditions[d]
(1)	(2)	(3)	(4)	(5)	(6)
Hya03	J04102390+1459104	2017 Feb 19th	2 × 1700	1.0	Clear
Hya08	J04584566+1212343	2017 Jan 27th	4 × 1700	0.5	Clear
Hya09	J04463535+1451261	2016 Dec 7th	2 × 1500	0.6	Spectroscopic
Hya09	J04463535+1451261	2017 Dec 25th	4 × 2000	1.1	Clear
Hya10	J04173397+1430154	2018 Jan 9th	2 × 1800	1.1	Clear
Hya11	J03554191+2257016	2016 Dec 7th	2 × 1500	0.5	Spectroscopic
Hya11	J03554191+2257016	2018 Jan 9th	2 × 1800	1.1	Clear
Hya12	J04354302+1323448	2017 Dec 24th	4 × 2000	0.7	Clear
DENIS-P J0615−01	J06154934−0100415	2016 Dec 9th	2 × 900	0.8	Spectroscopic

Notes.
[a] Names of Hyades L dwarfs from Hogan et al. (2008).
[b] Number of exposures × on-target exposure time.
[c] Values taken from GTC log of observations.
[d] Sky conditions reported by the night observers. Spectroscopic means that some clouds were passing during the night.

Table 2
Hyades Sample Properties

Name	*SpT*	D_{spec}[a] (pc)	$\log(L_{bol}/L_{\odot})$[b]	T_{eff}[b] (K)	RV (km s^{-1})	Memb.
(1)	(2)	(3)	(4)	(5)	(6)	(7)
Hya03	L2.0 ± 0.5	48 ± 9	−3.83 ± 0.13	1959 ± 113	24 ± 13	95%
Hya08	L2.0 ± 0.5	45 ± 9	−3.83 ± 0.13	1959 ± 113	23 ± 14	95%
Hya09	L3.5 ± 0.5	57 ± 8	−4.03 ± 0.13	1758 ± 113	45 ± 13	98%
Hya10	L3.5 ± 0.5	58 ± 8	−4.03 ± 0.13	1758 ± 113	48 ± 13	95%
Hya11	L3.0 ± 0.5	50 ± 7	−3.96 ± 0.13	1822 ± 113	45 ± 11	95%
Hya12	L4.0 ± 0.5	56 ± 8	−4.10 ± 0.13	1695 ± 113	36 ± 13	98%

Notes.
[a] Spectrophotometric distances derived from photometry in Hogan et al. (2008) and Lodieu et al. (2014) and the spectral type versus absolute magnitude relations for field L dwarfs (Filippazzo et al. 2015).
[b] Bolometric luminosities and effective temperatures estimated using the calibrations of those parameters with spectral type given in Filippazzo et al. (2015).

In Section 2, we present the target selection and the spectroscopic observations. In Section 3, we present the spectral types, spectrophotometric distances, and radial velocities of our targets, and we estimate their membership probability in the Hyades. We also derive astrophysical parameters such as bolometric luminosities and effective temperatures using empirical calibrations. In Section 4, we present the search for Li, as well as for Hα in emission, and we give the pseudo-equivalent width measurements of photospheric lines seen in the spectra. In Section 6, we discuss the determination of surface Li abundances in our sample of L dwarfs. Finally, in Section 6, we estimate the Hyades cluster age using the LDB method.

2. Target Selection and Spectroscopic Observations

We selected 6 targets from the list of 12 L-type Hyades BD candidates originally identified by Hogan et al. (2008) on the basis of photometric and proper motion criteria. These objects had been confirmed as L-type dwarfs from low-resolution optical spectra (Lodieu et al. 2014).

All of the spectra presented here were taken during dark nights in service mode at the 10.4 m Gran Telescopio Canarias (GTC) for programs GTC20-16B and GTC21-17B (PI, E. L. Martín) using the Optical System for Imaging and Low Resolution Integrated Spectroscopy (OSIRIS), Cepa et al. (2000). The instrumental configuration was the long slit mode with R1000R grating, a slit width of 1.2 arcsec, and a detector binning of 2 × 2. This combination gave a dispersion of 2.62 Å pixel^{-1}, and a resolving power ($R = \lambda/\Delta\lambda$) of 561 at the central wavelength of 743 nm, corresponding to a nominal FWHM resolution of 12 Å. The actual FWHM resolution of the spectra ranged from 10 to 12 Å according to measurements of sky airglow emission lines. The full spectral range of the data is from 510 to 1000 nm.

The observing sequences consisted of one direct imaging exposure to acquire the target (30 s or 50 s exposure times, depending on sky brightness, through the Sloan *z*-band), another exposure through the same filter to check centering on the slit, and several exposures in the long slit spectroscopic mode. An offset of 15 arcsec along the slit direction was applied between each exposure. All observations were carried out in parallactic angle.

As a radial velocity (RV) reference, the field L dwarf DENIS-P J0615493−010041 (Phan-Bao et al. 2008) was observed on 2016 December 9th. As this object is brighter ($I = 17.0$) than the Hyades targets, the exposure times were reduced to 20 s for the acquisition image and 900 s for each of the spectroscopic observations. Table 1 lists the targets observed for our lithium search and the observing details.

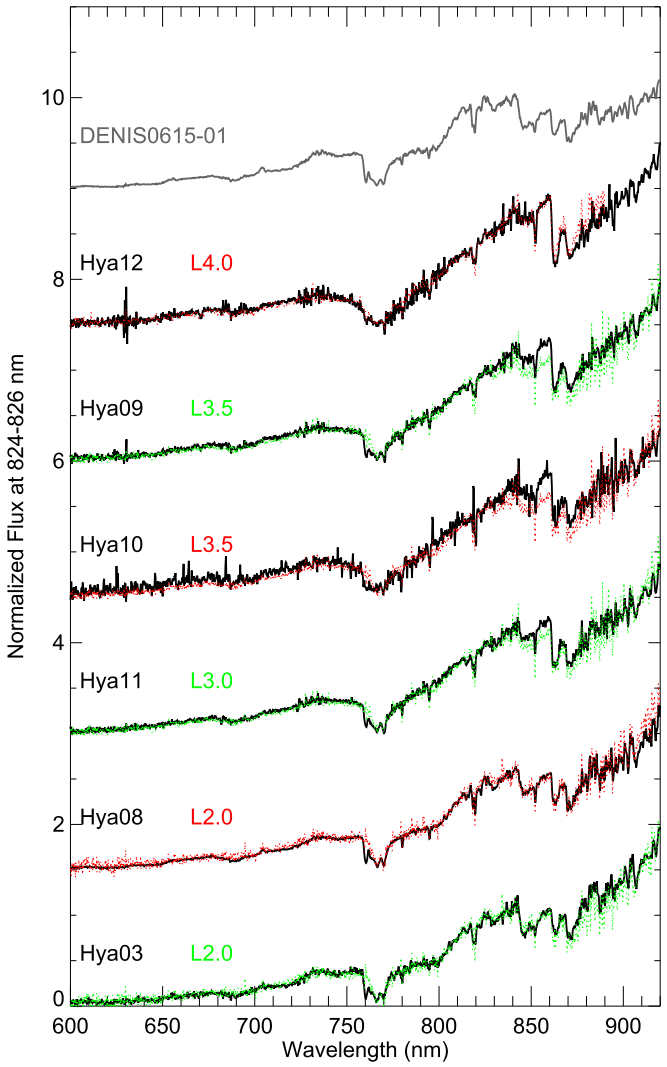

Figure 1. GTC/OSIRIS spectra of the Hyades L dwarfs observed in this work and the radial velocity standard. The best matching spectrum from the SDSS database is overplotted on each target and the spectral type of the template is labeled.

We used IRAF to reduce the data. Bias subtraction and flat field correction were performed. One-dimensional spectra were extracted interactively using apsum. Wavelength calibration was made using an arc lamp spectrum obtained the same night as the science spectrum. The spectrophotometric standard Hilt 600, observed with the same instrumental configuration in one of the same nights as the science spectra, was used to correct for instrumental response.

3. Cluster Membership

In Figure 1, we show the calibrated spectra of our targets compared with spectral templates from the Sloan Digital Sky Survey (SDSS; Schmidt et al. 2010) that provided the best match to our data. The spectral types adopted for our targets and their uncertainties are given in Table 2. Our spectral types are systematically later by 0.5–2.0 subclasses than those published by Lodieu et al. (2014), and consequently the spectrophotometric distances of the objects are closer and more consistent with cluster membership. On the other hand for DENIS J0615-010, we find a spectral type of L1 that is 1.5 subclasses earlier than the L2.5 type reported by Phan-Bao et al. (2008). Our spectral types ought to be more reliable than those estimated by other authors because of the higher quality of our data.

Spectrophometric distances were derived using the infrared photometry provided by Hogan et al. (2008) and Lodieu et al. (2014), and the spectral type versus absolute magnitudes for field L dwarfs in Filippazzo et al. (2015). They are given in Table 2. We note that they are consistent with the range of distances expected for cluster members, i.e., between 32 pc and 60 pc according to Hogan et al. (2008).

RV measurements were obtained for all the targets from cross correlation with the spectrum of the template DENIS J0615-010 using the IRAF task *fxcor*. Heliocentric radial velocity corrections were derived with the IRAF task *rvcor*. Instrumental zeropoint correction was applied using a radial velocity of $-21.0\,\mathrm{km\,s^{-1}}$ for DENIS J0615−010 (Burgasser et al. 2015). The measured radial velocities obtained for our targets and their uncertainties are provided in Table 2. The radial velocity values for all of our Hyades targets are consistent within the error bars with the *Hipparcos* mean value for the cluster ($39.5 \pm 0.3\,\mathrm{km\,s^{-1}}$) as provided by de Bruijne et al. (2011).

The contamination rate of the original sample of 12 Hyades L dwarf candidates discovered by Hogan et al. (2008) was estimated by those authors using comparison fields. They found that two candidates could be field M dwarfs, which was confirmed by Lodieu et al. (2014), who found that Hya05 and Hya07 are indeed field M dwarfs. Hya02 was reported not to be a BD by Casewell et al. (2014), but Lodieu et al. (2014) did confirm it as an L dwarf.

In order to estimate the membership probability of our targets in the cluster, we assume that contamination rate of two objects has a Poissonian error of ±1.4 objects. We assign a membership probability of 86% to each of the 10 Hyades L dwarf candidates found by Hogan et al. (2008) and confirmed as ultracool dwarfs by Lodieu et al. (2014), just based on the uncertainty in the contamination rate. To this probability, we add the fact that each one of our targets has an RV value and an uncertainty, and we estimate the probability that this value is just a chance coincidence with the cluster RV value. To perform this estimate, we use the distribution of RV measurements for L dwarfs provided by Burgasser et al. (2015). We find that among 21 L dwarfs with spectral subclass ranging from L1 to L5, one-third of them have RV values in the range 20 to $60\,\mathrm{km\,s^{-1}}$, which could be deemed as compatible with the cluster mean RV given the uncertainties of our RV measurements. Consequently, we increase the membership probability of our four targets from 86% to 95% because they have RV values consistent with the cluster within the measurement errors.

All BD evolutionary models predict that Li should be preserved at masses below $0.06\,M_{\odot}$, which corresponds to luminosities and temperatures in the realm of L dwarfs for ages younger than about 1 Gyr (D'Antona & Mazzitelli 1984; Burrows et al. 1997). The presence of Li is therefore an indication of younger age than the average for field L dwarfs. In the case of Hya09 and Hya12, we consider the presence of a detectable Li feature as an additional confirmation of membership in a cluster younger than the average age of the field population. Taking into account that the rate of Li detection in field L4 dwarfs is 40% ± 11% (Kirkpatrick et al. 2008), we add this factor to their membership probability. Thus, the Hyades membership probabilities of the six targets considered in this study include the facts that they have the correct

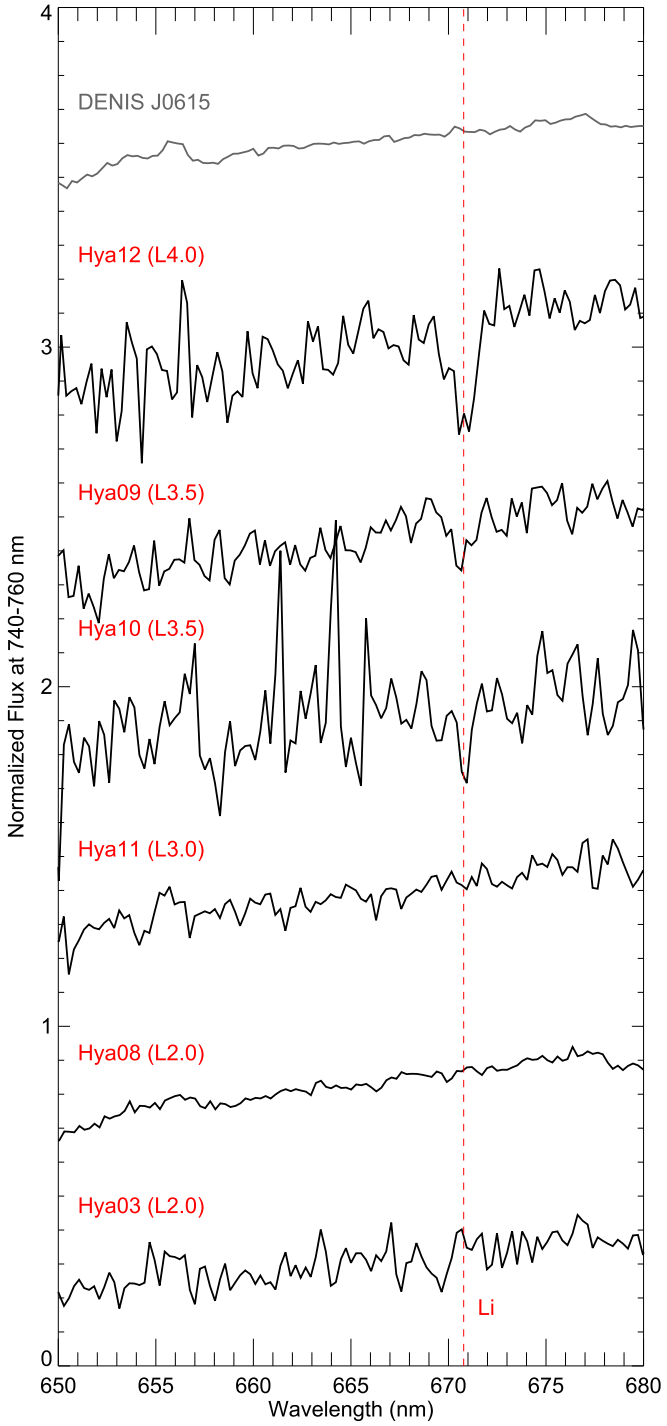

Figure 2. Zoom of the spectral region around the Li I resonance doublet at 670.8 nm. The central wavelength of the Li feature is marked with a dashed vertical line.

direction and magnitude of proper motion, the right spectral types and spectrophotometric distances, the correct location in color–magnitude diagrams, the correct radial velocity, and the presence of Li as an indicator of moderate youth and bona fide substellar status in the case of Hya09 and Hya12. They are listed in Table 2.

3.1. Astrophysical Parameters

None of our targets show spectroscopic signs of being very young (age < 100 Myr) as defined in Kirkpatrick et al. (2008). Their membership in the Hyades implies that they should have radii and surface gravities close to those of field L dwarfs. Therefore, it is justified to use the calibrations for field L dwarfs of known distance (Filippazzo et al. 2015) to calculate their bolometric luminosities ($\log(L_{\rm bol}/L_{\odot})$ and effective temperatures ($T_{\rm eff}$) from the spectral types obtained by us. They are given in Table 2.

We also tried other approaches, such as using the observed photometry and bolometric corrections from Filippazzo et al. (2015), and also Spectral Energy Distribution fitting with theoretical spectra following the procedures available in VOSA (Bayo et al. 2008), an interactive sofware developed by the Spanish Virtual Observatory. These other approaches gave larger uncertainties and they could be affected by unresolved binarity of the targets, which is known to be at least 10% among BDs in the Pleiades clusters (Martín et al. 2003; Bouy et al. 2006).

The advantage of using directly the calibrations between spectral type and luminosity and temperature is that the results do not depend on the distance nor on the appartent brightness of the objects. Thus, we adopt those values for the analysis of the LDB in the Hyades.

4. Atomic Lines

We searched for the Li I resonance doublet at 670.8 nm in all of the targets and did find something in three latest objects, namely Hya09, Hya11, and Hya12, as shown in Figure 2. The significance of these detections was estimated using the equation from Cayrel (1988); namely, $\mathrm{rms(pEW)} = 1.6 \times (\mathrm{FWHM} \times \mathrm{Disp.})^{1/2} \mathrm{S/N}^{-1}$ where in our case the following parameters apply: FWHM $= 12$ Å, Disp. $= 2.62$ Å pix^{-1}, and the signal-to-noise ratio (S/N) per pixel for each spectrum was computed using the key m in the IRAF task splot across the wavelength range from 675 to 680 nm. These S/N estimates were more conservative than those found using other methods.

In the case of Hya09, we found a predicted rms(pEW) for the Li I resonance doublet at 670.78 nm of 0.71 Å, which formally implies a significance of $6.2 \pm 0.7\sigma$ for the detection of this feature with a pEW $= 4.4 \pm 0.5$ Å. Hya10 has the poorest S/N of our sample and the predicted rms(pEW) for the Li I resonance doublet from the Cayrel equation is 1.45 Å. We do find a feature with a pEW of 3.2 ± 0.8 Å at the position of the Li I resonance doublet, but the significance is just $2.2 \pm 0.6\sigma$, and hence we cannot claim to have a definitive Li detection in Hya10. On the other hand, Hya12 has a Li I feature with a pEW $= 8.5 \pm 0.4$ Å, which implies a confidence of $13.3 \pm 0.7\sigma$ for this detection given than the predicted rms(pEW) is just 0.64 Å, and it is indeed the clearest Li detection in our whole sample. For the remainder of this paper, we will consider as definitive Li detections only the features observed in Hya09 and Hya12, while the rest will be treated as upper limits. As a consistency check, we also note that the FWHM of the Li I feature in Hya09 and Hya12 were consistent with the expected FWHM resolution as measured in other photospheric lines.

Independent measurements of the pEW for the Li I features by all the co-authors of this work using the task splot confirmed that the uncertainties estimated from the Cayrel formula are realistic; although, the interactive measurements tended to provide slightly higher error bars. Thus, we have adopted the more conservative uncertainties provided by the independent

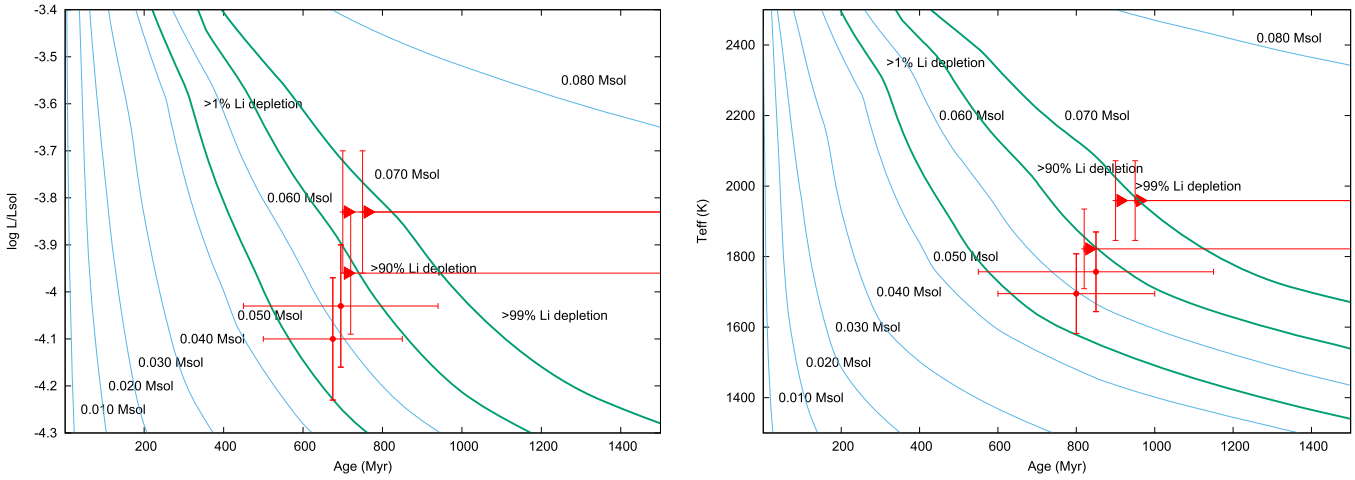

Figure 3. Evolutionary tracks for very low-mass stars and brown dwarfs as a function of age computed by Burrows et al. (1997). Masses and predicted Li depletion factors are labeled. The locations of the Hyades L dwarfs observed in this work are shown.

Table 3
Pseudo Equivalent Width Measurements[a]

Name	S/N 675–680 nm	pEW Hα 656.28 nm	pEW Li I 670.78 nm	pEW Rb I 780.03 nm	pEW Rb I 794.76 nm	pEW Na I 818.32, 819.48 nm	pEW Cs I 852.11 nm
(1)	(2)	(3)	(4)	(5)	(6)	(7)	(8)
Hya03	10.3	>-3.5	<0.5	2.5 ± 0.3	1.6 ± 0.3	5.7 ± 0.3	1.4 ± 0.2
Hya08	22.6	>-0.8	<0.3	2.8 ± 0.1	2.6 ± 0.2	4.8 ± 0.4	1.6 ± 0.1
Hya09	12.6	>-1.2	4.4 ± 0.5	2.7 ± 0.2	4.3 ± 0.3	4.3 ± 0.4	2.7 ± 0.1
Hya10	6.2	>-2.0	3.2 ± 0.8	2.6 ± 0.3	4.2 ± 0.4	5.6 ± 0.6	2.0 ± 0.1
Hya11	10.6	>-2.7	<0.8	2.4 ± 0.2	3.7 ± 0.2	4.1 ± 0.3	2.2 ± 0.1
Hya12	13.9	>-2.8	8.5 ± 0.4	8.0 ± 1.0	6.0 ± 0.7	5.0 ± 0.3	3.7 ± 0.1
D J0615-01	28.5	-2.3 ± 0.2	<0.1	2.7 ± 0.1	2.6 ± 0.2	6.7 ± 0.3	1.6 ± 0.2

Note.
[a] pEW measurements are given in Å.

measurements and they are given in Table 3. Table 3 summarizes the pEW measurements, upper limits, and uncertainties.

We also searched for Hα in emission, an indicator of chromospheric activity, but we could not find any clear detection among the Hyades L dwarfs. Upper limits to the Hα pEW are given in Table 3. None of our Hyades targets have Hα emission with pEW larger than about 4 Å, which is consistent with recent estimates of about 10% Hα emission detection rate among field L dwarfs (Pineda et al. 2016).

Prominent photospheric lines in L dwarfs of Cs I, Na I, and Rb I were present in the observed spectral range. Their pEWs were measured in a manner analog to that described for the Li I resonance feature. The line wavelengths listed in the NIST Atomic Spectra Database (Kramida 2007) and the pEWs that we measured are given in Table 3. For most of the lines, there is good agreement between our pEWs and those listed in Burgasser et al. (2015) for DENIS J0615−010, with the notable exception of the Na I doublet for which the pEWs in the literature are much weaker. This is likely due to the much higher spectral resolution ($R \sim 4100$) of the data reported in Burgasser et al. (2015), and highlights the importance of using data of similar resolution when comparing pEW values. We also note that the Cs I resonance line at 852.11 nm is stronger in Hya12 than in the other objects. This line is known to be very sensitive to $T_{\rm eff}$ in L dwarfs, becoming stronger for cooler and later objects (Kirkpatrick et al. 1999; Martín et al. 1999; Basri et al. 2000), which is consistent with Hya12 being the coolest L dwarf in our sample.

5. Lithium Abundances in Hyades L Dwarfs

Previous studies of the LDB in young open clusters and associations did not attempt to estimate surface Li abundances because the gap in luminosity across the LDB was comparable to observational uncertainties. However, for increasing age the gap in luminosity from Li bearing BDs to Li naked BDs becomes larger (Figure 3) and this motivated us to estimate the Li abundances in our targets. We calculated theoretical pEWs for the Li I resonance doublet using synthetic spectra for a range of $T_{\rm eff}$, log g and log N(Li) values that are relevant for our targets. The model names used in Table 4 denote the $T_{\rm eff}$ in K and log g adopted.

The theoretical spectra were synthesized following the procedures described in Lodieu et al. (2015). Fluxes across the Li I resonance doublet are governed mainly by absorption in the extended wings of the K I and Na I resonance lines (Pavlenko et al. 2000). The TiO bands are of marginal strength in L dwarfs. In our computations, only depletion of atomic lithium into molecular species (LiOH, LiCl, LiF) was accounted for. Depletion of lithium atoms into dust particles may reduce the number of absorbing particles in the

Table 4
Predicted Li Abundance vs. Relative pEW Li I

Model (1)	$\Delta\log N(\mathrm{Li})$ (2)	$(\mathrm{pEW\ Li\ I})_{\mathrm{depl}}/(\mathrm{pEW\ Li\ I})_{\mathrm{max}}$ (3)
1600/5.0	−0.5	0.57
1600/5.0	−1.0	0.32
1600/5.0	−1.5	0.18
1600/5.0	−2.0	0.10
1600/5.0	−2.5	0.06
1600/5.0	−3.0	0.04
1600/4.5	−0.5	0.57
1600/4.5	−1.0	0.33
1600/4.5	−2.0	0.11
1600/4.5	−3.0	0.04
1800/5.0	−0.5	0.57
1800/5.0	−1.0	0.33
1800/5.0	−1.5	0.19
1800/5.0	−2.0	0.11
1800/5.0	−2.5	0.07
1800/5.0	−3.0	0.04
1800/4.5	−0.5	0.58
1800/4.5	−1.0	0.33
1800/4.5	−1.5	0.19
1800/4.5	−2.0	0.11
1800/4.5	−2.5	0.07
1800/4.5	−3.0	0.04
1800/4.5	−3.5	0.03
1800/4.5	−4.0	0.02
2000/5.0	−0.5	0.57
2000/5.0	−1.5	0.19
2000/5.0	−2.0	0.11
2200/5.0	−0.5	0.58
2200/5.0	−1.5	0.19
2200/5.0	−2.0	0.11

Table 5
Li Depletion in Hyades L Dwarfs

Name (1)	*SpT* (2)	$(\mathrm{pEW\ Li\ I})_{\mathrm{obs}}/(\mathrm{pEW\ Li\ I})_{\mathrm{max}}$ (3)	$\log N(\mathrm{Li})$ (4)
Hya03	L2.0 ± 0.5	<0.06	<0.8
Hya08	L2.0 ± 0.5	<0.04	<0.3
Hya09	L3.5 ± 0.5	0.6 ± 0.4	2.8 ± 0.5
Hya10	L3.5 ± 0.5	<1	<3.3
Hya11	L3.0 ± 0.5	<0.11	<1.3
Hya12	L4.0 ± 0.5	0.8 ± 0.2	3.0 ± 0.3

atmosphere. Unfortunately, chemistry and kinematic properties of phase transition gas-dust are too poorly known to account for this effect.

Hyades BDs presumably start off their evolution with an initial Li abundance of log $N(\mathrm{Li}) \approx 3.3$ (in the scale log N (H) = 12.0), which is common among newly born stars (Bonsack & Greenstein 1960; Basri et al. 1991) and A- and F-type cluster members (Cummings et al. 2017). A high Li abundance of log $N(\mathrm{Li}) = 3.25 \pm 0.25$ has been inferred from self-consistent analysis of spectra of the field M9.5 BD LP944-20 (Pavlenko et al. 2007), which has an age estimated to lie in the range 475–650 Myr (Tinney 1998).

Assuming an initial Li abundance of log $N(\mathrm{Li}) = 3.3$, we find that the predicted Li pEW values from the synthetic spectra are larger by a factor of 1.7 ± 0.3 than the upper envelope of pEWs of the Li I feature reported among L1.5–L4.5 dwarfs, which is located between 8 and 15 Å (Kirkpatrick et al. 2000; Cruz et al. 2009; Lodieu et al. 2015). It is likely that the synthetic spectra overpredict the strength of the Li I feature because they do not include the effects of Li depletion into dust grains. In order to circumvent this problem, we adopt the upper envelope of observed Li I as representative of the initial Li abundance in L dwarfs. We use the synthetic spectra to calculate the relation between Li depletion due to Li burning and the ratio of the pEW of the Li I feature with respect to the maximum value, which corresponds to undepleted Li abundance. These relations are provided in Table 4, and we note that they are rather insensitive to the T_{eff} and log g adopted in the range of values considered in this work.

From the pEW values given in Table 3 and the calculations presented in Table 4, we derive the surface lithium abundances for our targets that are given in Table 5, assuming an undepleted Li abundance of log $N(\mathrm{Li}) = 3.3$. In particular, for an L4 dwarf (the spectral type of Hya12), we assume that the initial Li abundance corresponds to pEW $(\mathrm{Li\ I})_{\mathrm{obs}} = 11 \pm 4$ Å, and thus the pEW (Li I) measured in Hya12 is a factor of 1.3 ± 0.3 lower, which corresponds to a Li depletion of $\Delta\log N(\mathrm{Li}) = -0.3 \pm 0.3$ using the relations given in Table 4. Using log $N(\mathrm{Li}) = 3.3$ as the initial Li abundance for the Hyades, we obtain a surface Li abundance of log $N(\mathrm{Li}) = 3.0 \pm 0.3$ for Hya12, which could be consistent with complete Li preservation in this object. On the other hand, for an L3.5 dwarf (the spectral type of Hya09) we assume that the initial Li abundance corresponds to pEW $(\mathrm{Li\ I})_{\mathrm{obs}} = 7 \pm 4$ Å, and thus the pEW (Li I) measured in Hya09 is a factor of 1.6 ± 0.6 lower, which corresponds to a Li depletion of $\Delta\log N(\mathrm{Li}) = -0.5 \pm 0.5$ using the relations given in Table 4. Using log $N(\mathrm{Li}) = 3.3$ as the initial Li abundance for the Hyades, we obtain a surface Li abundance of log $N(\mathrm{Li}) = 2.8 \pm 0.5$ for Hya09, which is also consistent with no depletion at all, although with higher uncertainty than in the case of Hya12.

6. The Hyades Age

Given the bolometric luminosity, the effective temperature and the lithium abundance of an L dwarf, it should be possible to determine its age and mass, or place lower limits on them, using evolutionary models. Our goal in this section is to combine the Li abundances and upper limits derived in our sample of L dwarfs to check whether or not we can find consistent age estimates for all of them using two independent sets of models, namely those from Burrows et al. (1997) (hereafter Bu97) and those by Baraffe et al. (2015) (hereafter BHAC15).

The predicted relations between Li depletion and luminosity or temperature for these two models are shown in Figures 3 and 4, respectively. The age limits obtained for the five Hyades L dwarfs from comparison of their luminosities, T_{eff}, and Li abundances with the two sets of models are given in Table 6. Hya10 is not included because it does not provide any additional constraint.

Using the luminosities and the Bu97 models, we obtain a cluster age of 800 ± 50 Myr. Using the temperatures, the same models yield 975 ± 25 Myr. On the other hand, the BHAC15 models give 635 ± 85 Myr with the luminosities and 690 ± 110 Myr with the temperatures. Thus, there is a

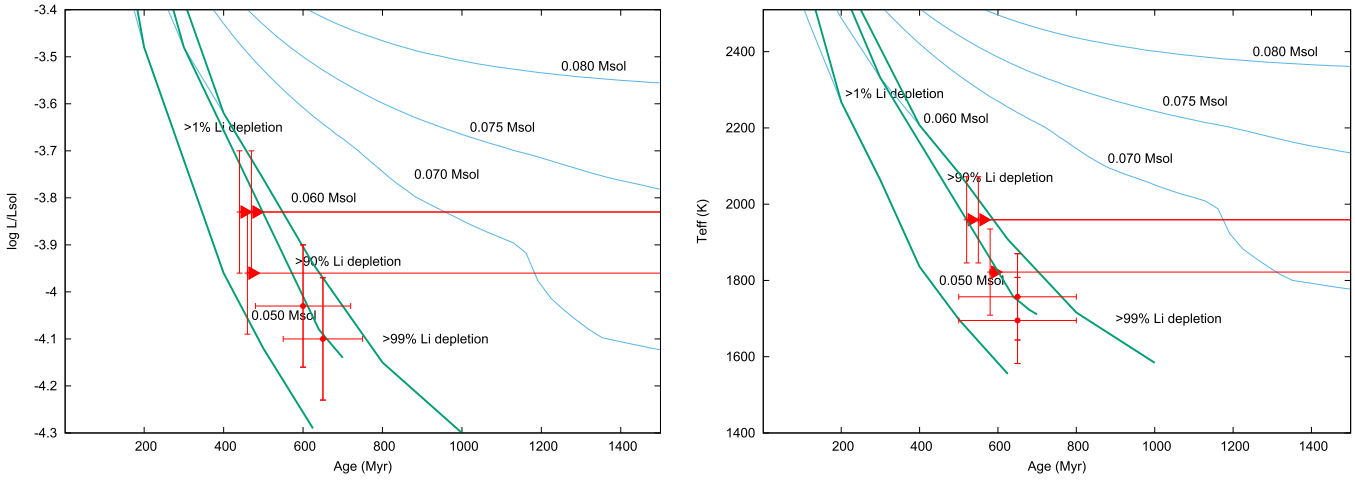

Figure 4. Evolutionary tracks for very low-mass stars and brown dwarfs as a function of age computed by Baraffe et al. (2015). Masses and predicted Li depletion factors are labeled. The locations of the Hyades L dwarfs observed in this work are shown.

Table 6
LDB Age Constraints for Hyades L Dwarfs

Name	$\log(L_{bol}/L_{\odot})$	T_{eff} K	Li Depletion	Age1 Myr Bu97-L	Age2 Myr Bu97-T	Age3 Myr Ba15-L	Age4 Myr Ba15-T
(1)	(2)	(3)	(4)	(5)	(6)	(7)	(8)
Hya03	−3.83 ± 0.13	1959 ± 113	>99.0%	>700	>900	>440	>520
Hya08	−3.83 ± 0.13	1959 ± 113	>99.9%	>750	>950	>470	>550
Hya09	−4.03 ± 0.13	1758 ± 113	0%–90%	450–940	550–1150	480–720	500–800
Hya11	−3.96 ± 0.13	1822 ± 113	>95.0%	>720	>820	>460	>580
Hya12	−4.10 ± 0.13	1695 ± 113	0%–78%	500–850	600–1000	550–750	500–800

significant region of agreement between the ages obtained from the BHAC15 luminosity tracks and the BHAC15 cooling curves, which is not the case for the Bu97 models. This lack of self-consistency in the Bu97 models could be due to the fact that they were mainly aimed at modeling in detail the properties of BDs cooler than 1300 K, whereas, for hotter BDs, such as those considered in this work, they use gray atmosphere approximations. The BHAC15 models, on the other hand, use detailed model atmospheres in the range of T_{eff} values considered in this work, and we adopt them for estimating the Hyades LDB age.

Assuming that the Hyades cluster is a coeval population of stars and BDs, it is found that an age of 650 ± 70 Myr provides a consistent description of our results using the BHAC15 models. This result is in excellent agreement with the canonical Hyades age of 625 ± 50 Myr (Maeder & Mermilliod 1981), although it does not rule out a slightly older age, which may be consistent within the error bars with the age of 750 ± 100 Myr suggested by models that incorporate the effects of stellar rotation (Brandt & Huang 2015).

The study of the LDB in the Hyades has some advantages and some disadvantages with respect to analog studies in younger clusters such as the Pleiades. On the positive side, the LDB in the Hyades is less prone to magnetic activity effects because L dwarfs are less active than late-M dwarfs, and thus no activity corrections have been attempted in this work for the Hyades, whereas in younger clusters, they have been deemed to be necessary (Juarez et al. 2014; Dahm 2015). Another bonus is that beyond 500 Myr, the location of the LDB depends primarily on the cluster age and almost nothing on the mass of the BDs. On the other hand, the effects of dust condensation in L-type atmospheres and how they may impact on the observational properties of L dwarfs and the determination of the LDB are complicated, and it could be worthwhile to investigate them in greater detail.

We thank the staff of the GTC who carried out the observations with OSIRIS in service mode for programs GTC20-16B and GTC21-17B, and I. Baraffe for providing a finer sampling of the Li depletion models for ages between 500 Myr and 700 Myr. E.L.M, N.L., and V.J.SB. are supported by grants AyA2015-69350-C3-1-P and AyA2015-69350-C3-2-P from the Spanish Ministry of Economy and Competitiveness (MINECO/FEDER). This publication makes use of VOSA, developed under the Spanish Virtual Observatory project supported from the Spanish MICINN through grant AyA2011-24052. We thank the anonymous referee for numerous comments that helped to improve this manuscript.

Facility: GTC(OSIRIS).

Software: IRAF (Tody 1986) VOSA (Bayo et al. 2008).

ORCID iDs

Eduardo L. Martín https://orcid.org/0000-0002-1208-4833
Nicolas Lodieu https://orcid.org/0000-0002-3612-8968

References

Baraffe, I., Homeier, D., Allard, F., et al. 2015, A&A, 577, 42
Barrado y Navascués, D., Stauffer, J. R., & Jayawardhana, R. 2004, ApJ, 614, 386

Basri, G., Marcy, G. W., & Graham, J. R. 1996, ApJ, 458, 600
Basri, G., Martín, E. L., & Bertout, C. 1991, A&A, 252, 625
Basri, G., Mohanty, S., Allard, F., et al. 2000, ApJ, 538, 363
Bayo, A., Rodrigo, C., Barrado y Navascués, D., et al. 2008, A&A, 492, 277
Bonsack, W. K., & Greenstein, J. L. 1960, ApJ, 131, 83
Bouvier, J., Kendall, T., Meeus, G., et al. 2008, A&A, 481, 661
Bouy, H., Moraux, E., Bouvier, J., et al. 2006, ApJ, 637, 1056
Brandt, T. D., & Huang, C. X. 2015, ApJ, 807, 58
Burgasser, A. J., Logsdon, S. E., Gagné, J., et al. 2015, ApJS, 220, 18
Burke, Ch. J., Pinsonneault, M. H., & Sills, A. 2004, ApJ, 604, 272
Burrows, A., Marley, M., Hubbard, W. B., et al. 1997, ApJ, 491, 856
Cargile, P. A., James, D. J., & Jeffries, R. D. 2010, ApJL, 725, L111
Casewell, S. L., Littlefair, S. P., Burleigh, M. R., et al. 2014, MNRAS, 441, 2644
Cayrel, R. 1988, in Proc. 132nd Symp. IAU, The Impact of Very High S/N Spectroscopy on Stellar Physics, ed. G. Cayrel de Strobel & M. Spite (Dordrecht: Kluwer), 345
Cepa, J., Aguiar, M., Escalera, V. J., et al. 2000, Proc. SPIE, 4008, 623
Cruz, K. L., Kirkpatrick, J. D., & Burgasser, A. J. 2009, AJ, 137, 3345
Cummings, J. D., Deliyannis, C. P., Maderak, R. M., et al. 2017, AJ, 153, 128
Dahm, S. E. 2015, ApJ, 813, 108
D'Antona, F., & Mazzitelli, I. 1984, ApJS, 491, 856
de Bruijne, J. H. J., Hoogerwef, R., & de Zeuuw, P. T. 2011, A&A, 367, 111
Dobbie, P. D., Lodieu, N., & Sharp, R. G. 2010, MNRAS, 409, 1002
Eggen, O. J. 1998, AJ, 116, 284
Filippazzo, J. C., Rice, E. L., Faherty, J., et al. 2015, ApJ, 810, 158
Hogan, E., Jameson, R. F., Casewell, S. L., et al. 2008, MNRAS, 388, 495
Jeffries, R. D., Naylor, T., Mayne, N. J., et al. 2013, MNRAS, 434, 2438
Juarez, A. J., Cargile, P. A., James, D. J., & Stassun, K. J. 2014, ApJ, 795, 143
Kirkpatrick, J. D., Cruz, K. L., Barman, T. S., et al. 2008, ApJ, 689, 1295
Kirkpatrick, J. D., Reid, N. I., Liebert, J., et al. 1999, ApJ, 519, 802
Kirkpatrick, J. D., Reid, N. I., Liebert, J., et al. 2000, AJ, 120, 447
Kramida, A. 2007, APS 38th Annual Meeting of the Division of Atomic, Molecular, and Optical Physics (College Park, MD: APS), D1.035
Lodieu, N., Boudreault, S., & Béjar, V. J. S. 2014, MNRAS, 445, 3908
Lodieu, N., Zapatero Osorio, M. R., & Rebolo, R. 2015, A&A, 581, 73
Maeder, A., & Mermilliod, J. C. 1981, A&A, 93, 136
Magazzù, A., Martín, E. L., & Rebolo, R. 1993, ApJL, 404, L17
Martín, E. L., Barrado y Navascues, D., Baraffe, I., et al. 2003, ApJ, 594, 525
Martín, E. L., Delfosse, X., & Basri, G. 1999, AJ, 118, 2466
Martín, E. L., Rebolo, R., & Magazzù, A. 1994, ApJ, 436, 262
Mazzei, P., & Pigatto, L. 1988, A&A, 193, 148
Pavlenko, Ya., Jones, H. R. A., Martín, E. L., et al. 2007, MNRAS, 380, 1285
Pavlenko, Ya., Zapatero Osorio, M. R., & Rebolo, R. 2000, A&A, 355, 245
Perez Garrido, A., Lodieu, N., & Rebolo, R. 2017, A&A, 599, 78
Phan-Bao, N., Bessell, M., Martín, E. L., et al. 2008, MNRAS, 383, 831
Phan-Bao, N., Bessell, M., Nguyen-Thanh, D., et al. 2017, A&A, 600, 19
Pineda, J. S., Hallinan, G., Kirkpatrick, J. D., et al. 2016, ApJ, 826, 73
Rebolo, R., Martín, E. L., Basri, G., et al. 1996, ApJL, 469, L53
Rebolo, R., Martín, E. L., & Magazzu, A. 1992, ApJL, 389, L83
Reid, N. 1992, MNRAS, 257, 257
Schmidt, S. J., West, A. A., Hawley, S. L., & Pineda, J. S. 2010, AJ, 139, 1808
Stauffer, J. R., Schultz, G., & Kirkpatrick, J. D. 1998, ApJL, 499, L199
Terlevich, E. 1987, MNRAS, 224, 193
Tinney, C. G. 1998, MNRAS, 296, L42
Tody, D. 1986, Proc. SPIE, 627, 733
van Leeuwen, F. 2009, A&A, 497, 209